

Stress-Induced Impairment of a Working Memory Task: Role of Spiking Rate and Spiking History Predicted Discharge

David M. Devilbiss*, Rick L. Jenison, Craig W. Berridge

University of Wisconsin-Madison, Madison, Wisconsin, United States of America

Abstract

Stress, pervasive in society, contributes to over half of all work place accidents a year and over time can contribute to a variety of psychiatric disorders including depression, schizophrenia, and post-traumatic stress disorder. Stress impairs higher cognitive processes, dependent on the prefrontal cortex (PFC) and that involve maintenance and integration of information over extended periods, including working memory and attention. Substantial evidence has demonstrated a relationship between patterns of PFC neuron spiking activity (action-potential discharge) and components of delayed-response tasks used to probe PFC-dependent cognitive function in rats and monkeys. During delay periods of these tasks, persistent spiking activity is posited to be essential for the maintenance of information for working memory and attention. However, the degree to which stress-induced impairment in PFC-dependent cognition involves changes in task-related spiking rates or the ability for PFC neurons to retain information over time remains unknown. In the current study, spiking activity was recorded from the medial PFC of rats performing a delayed-response task of working memory during acute noise stress (93 db). Spike history-predicted discharge (SHPD) for PFC neurons was quantified as a measure of the degree to which ongoing neuronal discharge can be predicted by past spiking activity and reflects the degree to which past information is retained by these neurons over time. We found that PFC neuron discharge is predicted by their past spiking patterns for nearly one second. Acute stress impaired SHPD, selectively during delay intervals of the task, and simultaneously impaired task performance. Despite the reduction in delay-related SHPD, stress increased delay-related spiking rates. These findings suggest that neural codes utilizing SHPD within PFC networks likely reflects an additional important neurophysiological mechanism for maintenance of past information over time. Stress-related impairment of this mechanism is posited to contribute to the cognition-impairing actions of stress.

Citation: Devilbiss DM, Jenison RL, Berridge CW (2012) Stress-Induced Impairment of a Working Memory Task: Role of Spiking Rate and Spiking History Predicted Discharge. *PLoS Comput Biol* 8(9): e1002681. doi:10.1371/journal.pcbi.1002681

Editor: Olaf Sporns, Indiana University, United States of America

Received: February 28, 2012; **Accepted:** July 19, 2012; **Published:** September 13, 2012

Copyright: © 2012 Devilbiss et al. This is an open-access article distributed under the terms of the Creative Commons Attribution License, which permits unrestricted use, distribution, and reproduction in any medium, provided the original author and source are credited.

Funding: The funding sources for this project were from NSF IOS-0918555 (DMD), NIH MH081843, DA00389, and NS032461 (CWB). The funders had no role in study design, data collection and analysis, decision to publish, or preparation of the manuscript.

Competing Interests: I have read the journal's policy and have the following potential conflicts: RLJ reports no conflict of interest. DMD is the founder of NexStep Biomarkers, LLC. NexStep Biomarkers had no role in study design, data collection and analysis, decision to publish, or preparation of the manuscript. NexStep Biomarkers, does not employ anyone who worked on this project, hold patents related to this project, sell products related to this project, or provided consultation on this project. This manuscript provides no financial gain for NexStep Biomarkers. Dr. Berridge has received expert witness fees from Teva Pharmaceutical, Activis, Aurobindo Pharmaceuticals, Mylan Pharmaceuticals, and Apotex.

* E-mail: ddevilbiss@wisc.edu

Introduction

The prefrontal cortex (PFC) plays a central role in a diverse set of cognitive and behavioral processes, including sustained attention, working memory, and behavioral inhibition. In rat, the prelimbic region of the PFC (plPFC) is a crucial subregion for these cognitive processes [1–4]. Delayed-response tasks of working memory have been extensively used to study the neurobiological basis of PFC-dependent function, in which information is retained during short delay intervals and used to guide subsequent behavior [5–11]. Seminal electrophysiological studies identified a subset of PFC neurons that display persistent spiking activity during delay periods of these tasks [7,12]. Spiking rates during delay periods are correlated with both specific task-related cues and the number of cues required to be maintained during the delay period. Based on these observations, delay-related spiking activity is posited to reflect the maintenance of attentional processes, abstract rules, or past stimuli and events [13–15]. Additional evidence indicates that

firing rates of PFC neurons during the response and reward phase of these tasks may reflect decision-related or reward/response outcome evaluation [12,13,16,17].

Currently there are competing hypotheses in the literature regarding the potential effects of stress on PFC spiking activity. One view proposes that stress related increases in norepinephrine (NE) α_1 - and dopamine (DA) D_1 -receptor signaling within the PFC will act to inhibit persistent spiking rates during delay intervals of these tasks [18]. In contrast, it is also posited that stress-related increases in glucocorticoid-receptor signaling will enhance spiking rates by facilitating or increasing glutamatergic neurotransmission [19–22]. NE, DA, and glucocorticoids activate multiple receptor subtypes, each producing complex concentration- and receptor-dependent modulatory actions on spiking activity of target neurons [22–30]. Moreover, the combined actions of these neuromodulators on target neuron spiking rates during stress are difficult to predict. Indirect evidence also predicts that during stress, high levels of NE and DA may act to disconnect

Author Summary

When faced with stressful situations, normal thought processes can be impaired including the ability to focus attention or make decisions requiring deep thought. These effects can result in accidents at the workplace and in combat, jeopardizing the lives of others. To date, the effect of stress on the way neurons communicate and represent cognitive functions is poorly understood. Differing theories have provided opposing predictions regarding the effects of stress-related chemical changes in the brain on neuronal activity of the prefrontal cortex (PFC). In this study, we show that stress increases the discharge rate of PFC neurons during planning and assessment phases of a task requiring the PFC. Additionally, using a point process model of neuronal activity we show that stress, nonetheless, impairs the ability of PFC neurons to retain representations of past events over time. Together these findings suggest that stress-related impairment of cognitive function may involve deficits in the ability of PFC neurons to retain information about past events beyond changes in neuronal firing rates. We believe that this advancement provides new insight into the neural codes of higher cognitive function that may lead to the development of novel treatments for stress-related diseases and conditions involving PFC-dependent cognitive impairment.

PFC neurons from excitatory recurrent feedback and suppress recursive, delay-related discharge of PFC neurons [18]. These actions are posited to involve the degradation of intrinsic neuronal mechanisms and excitatory recurrent neural connectivity that likely support the maintenance of information over time within PFC networks [2,31–37].

Although there exists a large body of evidence demonstrating that stress impairs higher cognitive processes dependent on the PFC [38–40], surprisingly, to date the actions of stress on PFC neuronal discharge in animals engaged in tasks of working memory remain unknown. To address this gap in our understanding, we examined the relationship between acute noise stress-related impairment of performance during a PFC-dependent T-maze based delayed-response task of spatial working memory and stress-related changes in p_{i} PFC neuronal spiking rates during the delay-period and other components of this task. Additionally, we directly determined the degree to which PFC neurons retain representations of past events over time by quantifying spike history-predicted discharge (SHPD) using a conditional intensity-generalized linear model statistical framework (CI-GLM) [41–45]. With the CI-GLM framework, we addressed several questions related to the actions of stress on PFC neuron function. First, to what degree does past spiking activity of PFC neurons predict or modulate ongoing activity of these neurons? Second, does stress have an overall impact on the predictability of PFC neuron discharge given a cell's intrinsic spiking history? Third, do specific task components (i.e. delay-period vs. behavioral response) interact with or modulate SHPD during baseline and acute stress? Combined, these studies represent a first characterization of the predictability of neural discharge from intrinsic spiking history within PFC networks of animals engaged in a cognitive task under normal and acute stress conditions.

Results

Characterization of Neural Recordings during a Working Memory Task

Five animals were tested in a T-maze based delayed-response task of spatial working memory (**Fig. 1** and **Fig. S2**). This task

has been previously shown to be dependent on a functionally intact PFC and require PFC-dependent cognitive processes [4,24,30,38]. In this task, animals were required to enter the T-maze arm opposite from the one last visited, following a delay period to obtain food rewards (chocolate chips 1.6 gm) delivered by the experimenter's hand. Delay length was specific to each animal (range 10–40 sec) and chosen to maintain baseline performance near 90% correct. Animals were tested for two sessions a day separated by two hours during which the animal remained tethered to the recording equipment. Each session consisted of 41 trials; the 1st trial of each session was always rewarded and not analyzed. During the first session (baseline), low-level masking white noise (60 db) was presented continuously and animals performed well (average 93% accuracy) with 3–4 errors occurring sporadically throughout the session (**Fig. 1B**). Intense white noise (93 db), presented throughout the second testing session, significantly impaired performance in this task, with animals performing at an average of 64.8% (–28%; $p < 0.0005$ pairwise t-test). Acute white noise is a well-characterized stressor that elicits the physiological responses of stress and impairs PFC-dependent cognitive function in both humans and animals [18,40,46–51].

In these same animals, bilateral implants of electrode arrays permitted simultaneous recordings of extracellular discharge activity from layer V of the p_{i} PFC yielding 491 spike trains from single neurons (**Fig. 1C–D**) [46,52]. A subset of 339 of these neurons were classified as “wide spike” (**WS-type**) based upon action potential features, thus putative glutamatergic pyramidal neurons [53], and exclusively used for these analyses. Analyses of spiking activity were limited to trials containing correct responses, given so few error trials occurred during baseline testing sessions and reliable estimates of neuronal spiking activity were difficult to obtain.

Effects of Stress on Delay- and Response-Related Discharge Rates in the p_{i} PFC

Discharge rates of WS-type p_{i} PFC neurons were characterized for intervals of the T-maze task (e.g. delay, run, and reward) using a peri-event time histogram (**PETH**) approach. Under baseline conditions, the discharge rate of p_{i} PFC neurons fluctuated throughout the time-course of each trial. The pattern of spiking activity was neuron-specific, with neurons exhibiting selective increases in discharge rate during single or adjacent behavioral intervals. A significantly large number of p_{i} PFC neurons exhibited delay-related spiking activity during baseline conditions (48.7%; $\chi^2 = 21.4$, $p < 0.001$). During delay periods, the discharge rates of these neurons averaged 0.55 Hz \pm 0.047 SEM. The illustrative cases shown in **Fig. 2A** demonstrate task-related fluctuations in discharge rate corresponding to delay periods, components of the behavioral response, and reward intervals across the recorded population of p_{i} PFC neurons during baseline sessions.

As illustrated by the examples shown in **Fig. 2B–D**, the effects of stress on p_{i} PFC neuron spiking rates were dependent on the behavioral intervals of the T-maze task. For these cases, stress increased delay-related activity 180% of baseline (0.018 to 0.033 Hz; **Fig. 2B**), whereas response related activity was suppressed during the run phase (42% of baseline, 0.092 to 0.039 Hz; **Fig. 2C**) with little effect during the choice phase (108% of baseline, 0.748 to 0.811 Hz; **Fig. 2D**). These opposing actions of stress on delay-related activity versus response-related activity were frequently observed across simultaneously recorded neurons within an animal. Within each component of the task, stress produced cell-specific modulatory actions on spiking rate of p_{i} PFC neurons, similar to prior reports on catecholamine

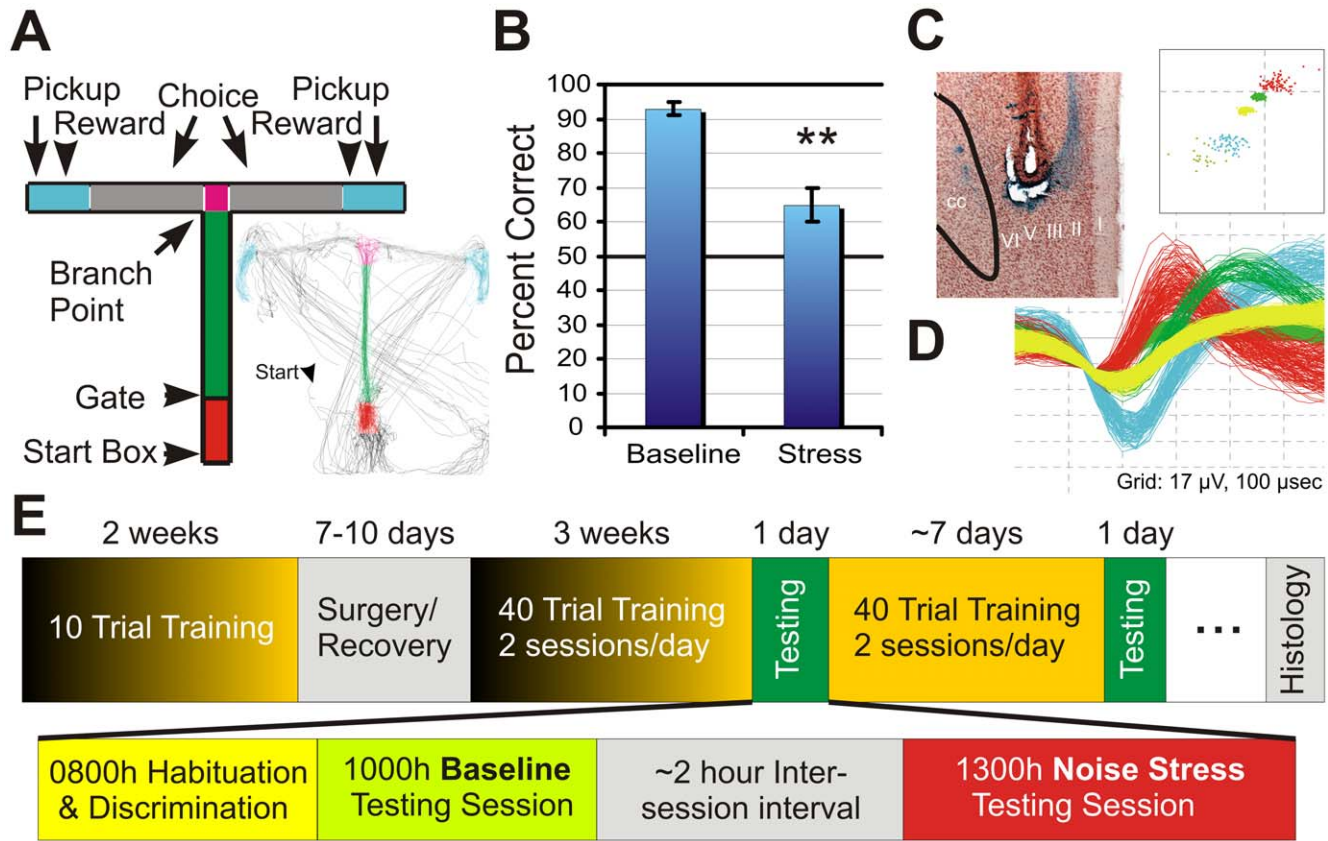


Figure 1. Electrophysiological recordings in rats performing the T-maze Task. **A**) Schematic of the T-Maze. On each trial, animals were placed in the start box (red) by the experimenter for a delay interval. The retaining gate was removed and the animal traveled to the branch point and revealed the choice to enter either arm (grey). Reward was then offered by the experimenter within the reward zone (cyan) if the arm opposite to the spatial location of last arm entered was chosen. Following reward or an incorrect choice, the animal was picked up by the experimenter and returned to the start box for a subsequent trial. **Inset** illustrates the video tracked path of a rat during one recording session. NOTE: paths crossing the T-maze from Pickup to Start Box reflect relocating the animal by the experimenter (right handed). **B**) Bar graph quantifying performance in the T-maze task during baseline and acute noise stress (93 db) conditions. $n = 5$; $**p < 0.01$. **C**) $40\times$ photomicrograph illustrating the final placement of one of eight microwires in layer V of the pPFC (Arrow Tip; CC, corpus callosum; pPFC, prelimbic PFC). **D**) Action potential waveforms of 5 discriminated and validated pPFC neurons. Waveform width = $450\ \mu\text{s}$. Waveforms from these units exhibited separable clusters when plotted in principal component space (inset). Sorted spiking activity with unsorted activity is presented in Fig. S1. The cyan colored neuron represents the characteristic WS-type neuron. **E**) Timeline of behavioral training and testing. Details of a single testing day are shown beginning at 8:00 AM. doi:10.1371/journal.pcbi.1002681.g001

neuromodulatory effects [25,29,52]. Nonetheless, across all recorded WS-type pPFC neurons, stress significantly affected task-related spiking rates of correct trials (rmANOVA(TaskComponent) $F_{(5,3810)} = 579.05$, $p < 0.0001$). During delay-periods, stress significantly *increased* the average discharge rate of these neurons (127% of baseline, **Fig. 3**). In contrast, stress *suppressed* the average spiking activity during the run and branch components of the behavioral response (78% and 92% of baseline respectively). During choice intervals, stress produced a modest increase in the average discharge rate (115% of baseline) but this effect was not statistically significant. Lastly, similar to that seen during the delay period, PFC neuron discharge rates during the reward and pickup components of the task were also facilitated by stress (135% and 130% of baseline). No differences were observed between the effects of stress on right vs. left trials. As such, these data suggest that intense acute stress generally enhances delay-related activity across PFC neurons. Moreover, the combined actions of acute stress across task intervals support the hypothesis that stress could differentially affect PFC-dependent processes that occur during the delay versus response period of these tasks.

Effects of Stress on Spike History-Predicted Discharge of pPFC Neurons

PFC neuron spiking activity during the T-maze task was further studied using CI-GLM's to assess whether SHPD significantly contributed to the ongoing activity of PFC neurons and the degree to which acute noise stress altered the predictability of PFC neuron discharge given a cell's intrinsic spiking history. The CI-GLM model (**1a**),

$$\lambda_{(Model\ 1a)}(t|H_t) = \exp\{\mu + \beta_1 X_t^{Baseline} + \vec{B}\vec{X}_t^{Interval} + \sum_{k=1}^{10} (\alpha_k X_t^{Baseline} + \eta_k X_t^{Stress}) \Delta N_{t-k}\},$$

included covariates representing the background level of spiking activity (intercept; μ), an index of baseline and auditory stress conditions within a testing day $\beta_1 X_t^{Baseline}$, the T-maze behavioral intervals (delay, run, branch, choice, reward, and pickup) $\vec{B}\vec{X}_t^{Interval}$, and a tenth order autoregressive process during baseline

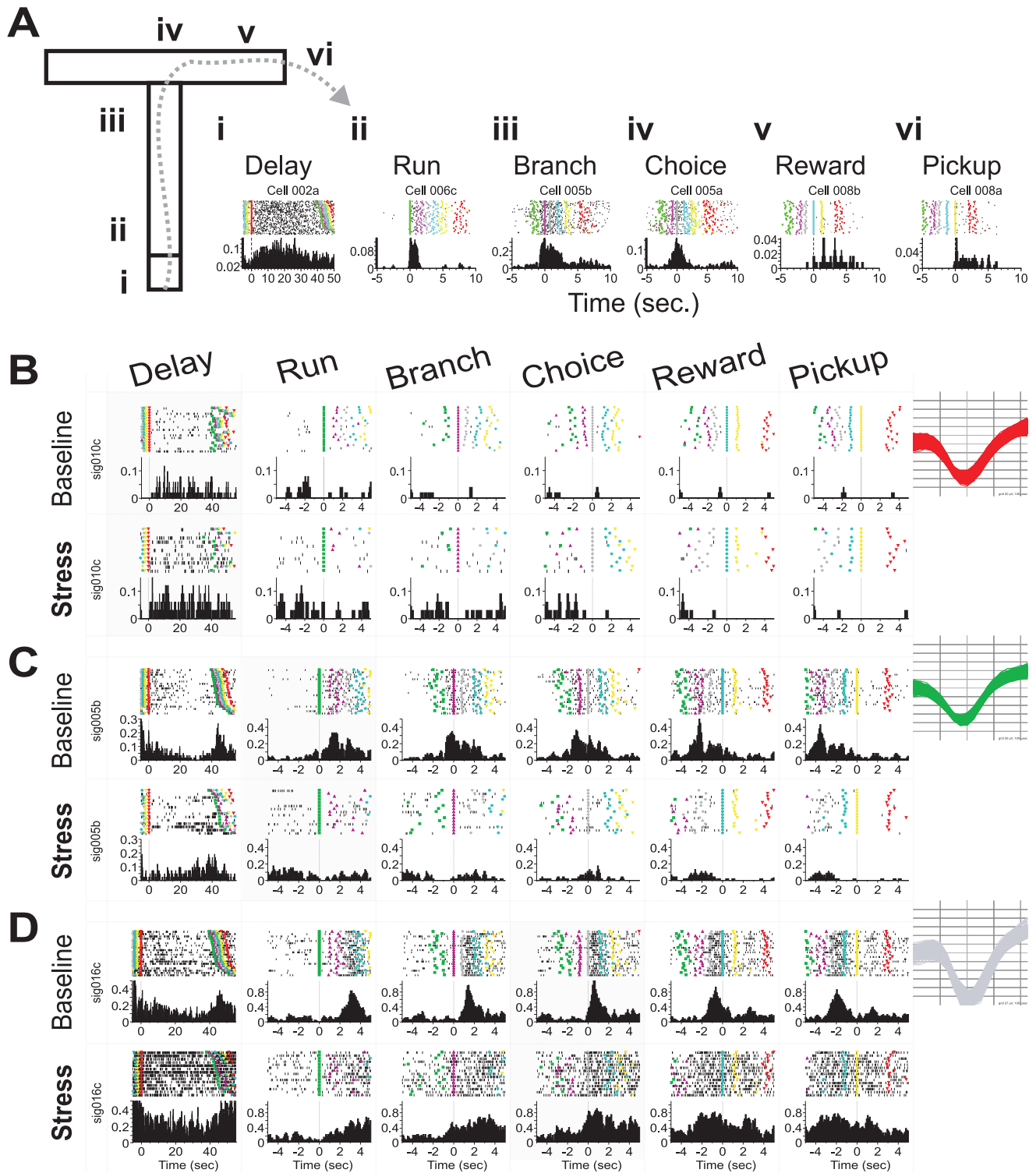


Figure 2. Peri-stimulus time histograms (PSTHs) illustrate the effects of stress on p PFC neuron task-related spiking activity. **A** T-maze schematic and associated peri-event raster and histogram analysis illustrates prototypic (i) delay- (ii) run- (iii) branch- (iv) choice- (v) reward- and (vi) pickup-related activity observed from p PFC neurons (0 sec. = start of respective behavioral interval; $n=40$ correct trials of a baseline recording session; Delay length = 20 sec.; 5 msec. bins). Colored fiduciaris indicate beginning of each major event of the T-maze task (Red, Start Box; Green, Gate; Magenta, Branch; Grey, Choice; Cyan, Reward; Yellow, Pickup). **B**) Task-related discharge of a single WS-type p PFC neuron during correctly executed trials with a left arm entry during the baseline recording session (17 trials; top) and subsequent stress session (11 trials; bottom). Delay-related spiking of this delay neuron was enhanced during stress. Inset illustrates recorded spike waveforms. PSTH y-axis represents spiking probability/bin normalizing for different numbers of trials (5 msec. bins). **C**) Run-related activity suppressed during stress conditions. **D**) Suppression of choice-related activity during stress. Labeling conventions of C–D are identical to B. doi:10.1371/journal.pcbi.1002681.g002

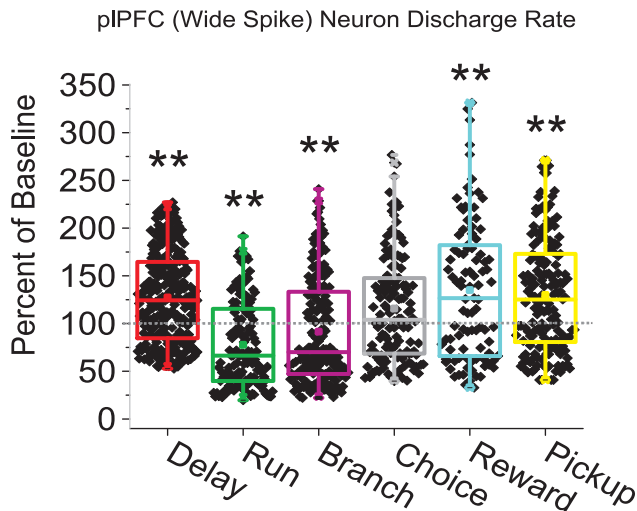


Figure 3. Effects of stress on task-related discharge rates of pIPFC neurons. Average discharge rates of WS-type pIPFC neurons during stress conditions were quantified for each behavioral interval of correct trials and plotted as a percent change from baseline conditions (1st recording session) for matched behavioral intervals trials with identical T-maze arm choices. Box and whisker plots illustrate that during stress, discharge rates within the Delay, Reward, and Pickup behavioral intervals are increased. During the Run and Branch behavioral intervals, discharge rates are suppressed under stress conditions. Colored box and whiskers designate the first and fourth quartiles and median line (box), distribution mean (dot), and 5–95% range of the data (whiskers). (**p < 0.01 FDR corrected T-Test compared to baseline).

doi:10.1371/journal.pcbi.1002681.g003

as well as during noise stress conditions $\sum_{k=1}^{10} (\alpha_k X_t^{Baseline} + \eta_k X_t^{Stress}) \Delta N_{t-k}$ with discretized time for increasing spike history durations represented as ΔN_{t-k} . Detailed descriptions of this and subsequent equations are presented in the Materials and Methods. From this model, the “spiking gain” of predicted discharge activity during baseline (α) and stress (η) conditions was calculated for each 250 ms bin back in time. Explicitly, the spiking gain is equivalent to the rate-ratio (exponentiated covariate weights i.e. α, η) [54] and represents the fold-change in predicted discharge activity given all other spiking activity occurring during the T-maze task.

Individual pIPFC neurons exhibited unique patterns of SHPD for each point back in time. For the illustrative cases shown in **Fig. 4A**, SHPD gains generally decayed with increasing time points in the past. Nonetheless, pIPFC neurons frequently demonstrated non-monotonic changes in SHPD gains at specific time points. For example, the highlighted pattern of SHPD gains of a single pIPFC neuron illustrates both a decay in SHPD gains over time and a selective increase in SHPD gain at 1.75 seconds. Similar to these individual cases the pattern of SHPD gains, averaged across the recorded population of WS-type neurons, decayed exponentially with increasing points further back in time during baseline conditions ($f_{(x)} = 1.16 + 0.544^{(-x/0.25)+0.51}$; **Fig. 4B**). Furthermore, although SHPD gains decayed over time, gains remained significantly greater than 1.0, indicating that spike history positively predicted future discharge for at least 2.5 seconds. Interestingly, the overall pattern of SHPD gains observed from pIPFC neurons differed from other areas of the cortex where SHPD does not significantly modulate ongoing spiking activity after 100 ms [55]. This difference may reflect unique intrinsic

neuronal or circuit properties of the PFC. Although acute noise stress did not alter the pattern of SHPD gains over time (ANOVA(Stress*Time) $F_{(9,3523)} = 0.86$, $p = 0.560$), stress did significantly reduce the magnitude of SHPD gains across all time intervals tested (ANOVA(Stress) $F_{(1,3523)} = 8.78$, $p = 0.0031$; **Fig. 4B inset**).

To confirm that task-related fluctuations in spiking rates were important to include in these models, Model 1a can be compared to the reduced model lacking T-maze behavior intervals covariates (i.e. $\lambda_{(Model1b)}(t|H_t) = \exp\{\mu + \beta_1 X_t^{Baseline} + \sum_{k=1}^{10} (\alpha_k X_t^{Baseline} + \eta_k X_t^{Stress}) \Delta N_{t-k}\}$). A comparison of these two models for each pIPFC neuron, demonstrated that the measure of deviance was significantly reduced for the majority of neurons (85.7%, 187 of 218 neurons; χ^2 test, FDR corrected p value < 0.0113) when CI-GLM’s included the T-maze behavior intervals (Model 1a). When analyses were replicated with the reduced model, a similar stressor-induced significant suppression of SHPD was found across individual pIPFC neurons (ANOVA(Stress) $F_{(1,4448)} = 19.71$, $p < 0.0001$; **Fig. S1**). Together these results support the general hypothesis that, in addition to task-related fluctuations in spiking rates, spike history plays an important role in shaping pIPFC neural discharge. Furthermore, the fact that stress suppressed SHPD in animals performing the PFC-dependent T-maze task likely suggests that SHPD may be an important mechanism supporting PFC-dependent cognitive functions. However, the degree to which these effects are specific to the T-maze task remains to be determined. Reverberations in recurrent cortical circuitry (**Fig. 4C**) or intrinsic neuronal mechanisms likely contribute to SHPD [31,35,39,56] and permit PFC neurons to maintain and preserve information within spiking patterns across large time intervals. However, the fact that stress did not alter the pattern of decay for SHPD gains throughout each trial suggests that stress may not change the underlying mechanism(s) generating SHPD.

Spike History-Predicted Discharge Is Selectively Impaired during Delay Intervals

Delay-related spiking activity is posited to serve a pivotal role in the accurate performance of delayed response tasks of working memory [2,3,18,30,57]. To determine if stress preferentially affects SHPD during delay intervals, a second CI-CLM was formulated to examine the interaction between spike history and the extended delay interval (Pickup-Delay; **Model 2**).

$$\lambda_{(Model2)}(t|H_t) = \exp\left\{\mu + \sum_{k=1}^{10} \gamma_k \Delta N_{t-k} + \beta_1 X_t^{Baseline} + \beta_2 X_t^{Delay} X_t^{Baseline} + \beta_3 X_t^{Delay} X_t^{Stress} + \sum_{k=1}^{10} (\alpha_k X_t^{Delay} X_t^{Baseline} + \eta_k X_t^{Delay} X_t^{Stress}) \Delta N_{t-k}\right\}.$$

This model included the intercept (μ), the main effects of SHPD $\sum_{k=1}^{10} \gamma_k \Delta N_{t-k}$, baseline and stress conditions within a testing day $\beta_1 X_t^{Baseline}$, and the first-order extended delay interval interaction $\beta_2 X_t^{Delay} X_t^{Baseline} + \beta_3 X_t^{Delay} X_t^{Stress}$. The second-order interaction terms of this model, $\sum_{k=1}^{10} (\alpha_k X_t^{Delay} X_t^{Baseline} + \eta_k X_t^{Delay} X_t^{Stress}) \Delta N_{t-k}$, correspond to delay-specific SHPD during baseline (α) or stress (η) conditions beyond the main effects of stress accounted

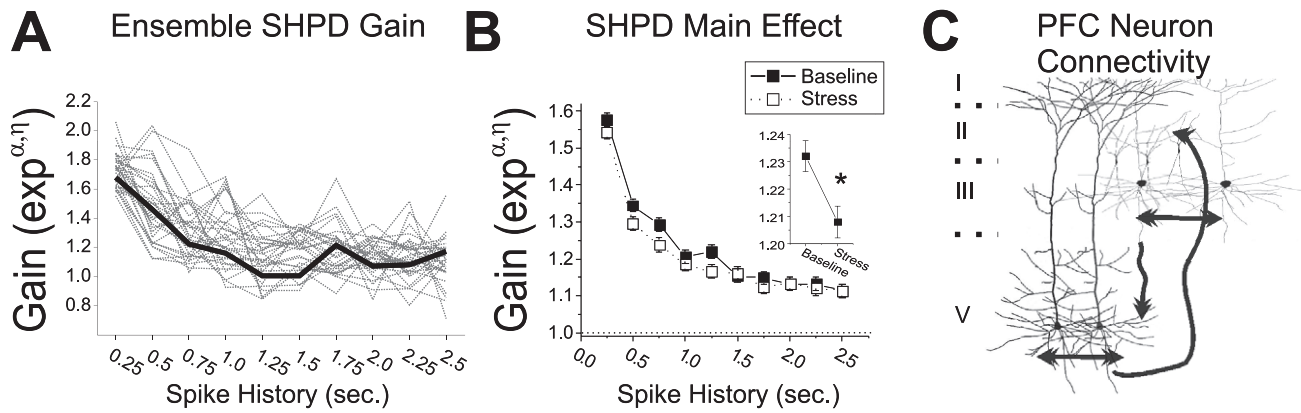


Figure 4. Stress-related changes in pPFC neuron spike-history predicted discharge (SHPD) throughout baseline or acute stress conditions. **A)** Spiking gain (rate-ratio $\exp^{\alpha,\eta}$) measures of the contribution of spike history at different points back in time for a small ($n=50$) ensemble of neurons. The SHPD gain of one exemplar neuron is highlighted. **B)** SHPD gain at different points back in time decay exponentially under baseline and stress conditions (Model 1a). Described in the main text, stress produced an overall reduction in SHPD gains (inset; $*p<0.005$), but did not significantly alter the decay of gains at any spike history time bin. **C)** Schematic of recurrent pathways within the PFC of connectivity within layers II/III or V as well as connectivity between II/III and V represents one putative mechanism supporting SHPD. Adopted from: [72–74]. doi:10.1371/journal.pcbi.1002681.g004

for in Models 1a,b. During baseline conditions, the gains of delay-specific, SHPD (α) averaged across all WS-type pPFC neurons were all positive and significantly greater than one (**Fig. 5A**). For the first 1.5 seconds of spiking history, gains were essentially flat and averaged 1.08 ± 0.0045 (SEM). During acute noise stress, gains for the most recent spike history intervals (η) were suppressed from baseline levels (ANOVA(Stress*Time) $F_{(9,4671)} = 2.00$, $p = 0.035$). Although stress-related suppression of delay-specific, SHPD gains was observed for intervals up to 1.5 seconds, a statistically significant difference from baseline levels was only observed at 0.5 and 1.25 seconds (FDR corrected). Moreover, delay-specific SHPD gains at the 1.25 second time point were not statistically different than 1.0 during conditions of noise stress. Given that the comparison between baseline and stress conditions was determined in the same CI-GLM, no deviance tests were performed. We posit that suppression of delay-specific SHPD of PFC neurons during conditions of stress contributes to stress-dependent impairment in delay-related PFC-dependent functions.

We next examined the interaction between spike history and the response interval (Run-Branch-Choice; **Model 3**):

$$\lambda_{(Model3)}(t|H_t) = \exp\left\{\mu + \sum_{k=1}^{10} \gamma_k \Delta N_{t-k} + \beta_1 X_t^{Baseline} + \beta_2 X_t^{Response} X_t^{Baseline} + \beta_3 X_t^{Response} X_t^{Stress} + \sum_{K=1}^{10} (\alpha_k X_t^{Response} X_t^{Baseline} + \eta_k X_t^{Response} X_t^{Stress}) \Delta N_{t-k}\right\}.$$

Similar to Model 2, gains associated with these model interaction terms represent response-specific gain of SHPD beyond the main effects of stress accounted for in Models 1a,b. Response-specific interaction term gains exhibited several important stress-related effects, even though these effects were more complex than the effects of stress on delay-specific interaction gains. First, during baseline recordings, response-related gains for intervals up to 1.0 second were not significantly different from one, making no contribution to the prediction of discharge activity (**Fig. 5B**). Stress significantly *increased* these response-specific SHPD gains at

0.25 and 0.75 second intervals (ANOVA(Stress*Time) $F_{(9,6894)} = 7.3$, $p < 0.0001$). Second, under baseline conditions spike history response-related gains at longer intervals increased gradually to become significantly different than one. Stress significantly reduced long spike history interval response-specific gains to values that were equivalent to one (1.75, 2.0, and 2.5 seconds). We posit that the different effects of stress, on delay-specific versus response-specific gain of SHPD, likely reflect differing roles for SHPD in the cognitive or behavioral processes that occur during these behavioral intervals.

Discussion

The present study characterized the actions of acute noise stress on discharge rate and SHPD of medial PFC neurons in rats engaged in a T-maze delayed-response task. This stressor impaired performance in this task and generally suppressed the ability for past spiking activity of PFC neurons to predict or modulate these neurons ongoing activity. We further demonstrate that the effects of stress on SHPD as well as discharge rate are dependent on specific phases of the task including the delay and response periods. During delay periods, stress suppressed SHPD of pPFC neurons and enhanced delay-related firing rates. Outside of the delay period, SHPD was increased during the response period associated with a suppression of spiking activity during these same conditions of stress. These observations begin to provide an important link between the well-documented effects of stress on PFC-dependent cognitive functions and the impact of stress on PFC neural codes during a delayed-response task used to probe PFC-dependent function. Combined, these studies identify broad effects of stress on PFC neuronal activity that likely represent key aspects of the neurophysiological bases of stress-related cognitive impairment.

Technical Considerations

The T-maze delayed alternation task embodies a number of important cognitive/behavioral processes and neurophysiological features associated with PFC function of human and non-human primates. This task is highly dependent on the PFC and sensitive to the effects of stress [30], similar to tasks used in humans to probe PFC function. Additionally, it is posited that the T-maze task

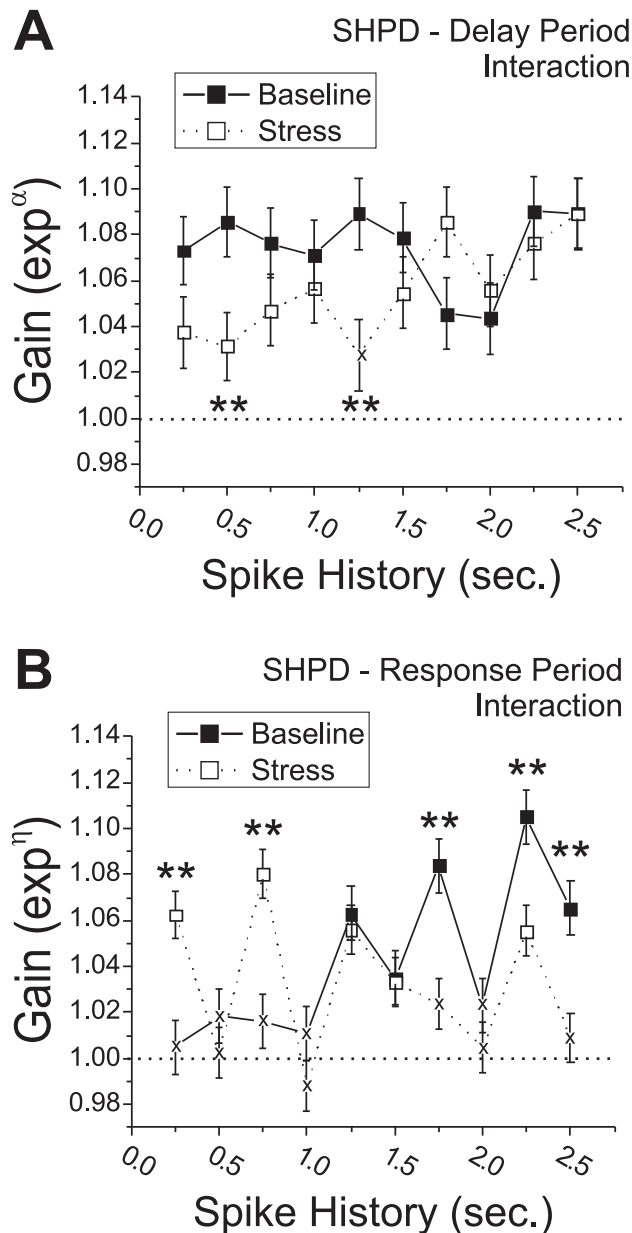


Figure 5. Stress-related changes in delay- and response-related p_{iPFC} neuron spike-history predicted discharge (SHPD). **A**) Delay-specific gains of SHPD interaction terms from the CI-GLM (Model 2; α , η) were averaged across p_{iPFC} neurons and plotted. **B**) Response interval-specific gains of SHPD interaction terms (Model 3). Stress suppressed delay-specific SHPD gains and increased the impact of the most recent spiking history during the response period. (* $p < 0.05$ FDR corrected compared to baseline; $x < 0.05$ FDR corrected compared to 1.0). doi:10.1371/journal.pcbi.1002681.g005

requires PFC-dependent processes including working memory, attention, inhibition of proactive interference, and inhibition of distracter interference (generated by handling the animal between each trial), similar to tasks used to probe PFC-dependent function in primates and humans [1,33,58,59]. In animals performing the T-maze task, we observed a significant number of PFC neurons exhibiting delay-related spiking activity, similar to that observed in primates performing delayed-response tasks [33,60,61]. More automated versions of these tasks, including the Figure-8 maze

task, lack distracter interference and possibly other processes requiring significant engagement of the PFC. Such differences between the T-maze task and Figure-8 tasks may explain why automated delayed-response tasks have shown only few delay-related cells in rodent PFC [62].

Intense white noise is a well-characterized audiogenic stressor that impairs working memory, attention, and other PFC-dependent functions in rats, monkeys, and humans [38,48,51,57,63]. In the current study, continuous presentation of intense white noise (93 db) impaired performance of the T-maze based delayed-response task of spatial working memory and increased PFC neuron firing rates during the delay period. Similar impairment in T-maze performance is seen when animals are exposed to restraint stress *immediately prior* to testing [64,65], but not after 4 hours of recovery from restraint stress [22]. Although previous studies have demonstrated that non-stressful white noise can activate PFC neurons [66], these cells are few in number (approximately 2% of PFC neurons). For these PFC neurons, responses to white noise are phasic, quickly adapting, and are linked to the onset of the stimuli. During presentation of noise stress in the current study, PFC neuron firing rates were increased during the delay period but, importantly, were suppressed during the behavioral response. Together, the above observations provide strong evidence that the effects of noise stress on PFC neuron spiking activity were not induced by a continued sensory response to intense white noise.

In the present study, a CI-GLM framework was used to examine the degree to which past spiking activity of p_{iPFC} neurons contributes to ongoing neural discharge patterns. Although the CI-GLM approach has been used successfully to distinguish between intrinsic spiking-history related discharge and extrinsic activity in motor cortex [67,68], here we extend its use to examine SHPD in PFC networks. An advantage of this approach over peri-event time histogram analysis or other univariate analyses, including autocorrelogram analysis, is that the CI-GLM approach can disambiguate the relative contributions of spiking history from that of experimental and task-related variables to spiking activity. In the current study, task- and stress-related changes in overall firing rates were captured in the β/B terms of the model separately from the effects of the interaction terms (α or η). Thus, SHPD during baseline could be directly compared to SHPD during stress conditions in a manner that accounted for the effects of stress on the overall discharge rate and task-related fluctuations in spiking activity within each trial. A second consideration for the CI-GLM approach is the use of a Poisson distribution to fit the CI-GLM to neural data over other distributions, including Gaussian or Bernoulli. By doing so, this does not imply that a Poisson process generates p_{iPFC} neuronal spiking activity. Instead, the Poisson distribution is the appropriate distribution for what is, in simplified terms, a spiking count-based multivariate regression and provides a computationally tractable solution to fit p_{iPFC} neuronal spiking activity. A number of excellent reviews described these statistical modeling methods and the appropriate use of these models to characterize spike trains (e.g. [45]).

The Role of Spike History in Cognitive Function

The present findings demonstrate that under baseline conditions, past spiking activity of a p_{iPFC} neuron positively predicts future neuronal discharge. The contribution of past spiking activity to ongoing discharge of p_{iPFC} neurons decayed exponentially with time during baseline and stress conditions; spiking-history at time points up to 1–1.5 seconds comprised most of the predictive power. With delay periods ranging from 10–40 seconds and behavioral responses lasting several seconds, we posit that the time

scale of SHPD is likely an important PFC neural process for the stable maintenance of information for short intervals during delay periods of working memory tasks while providing a mechanism that allows integration of new spiking activity patterns within PFC networks that permits flexible goal-directed behaviors. This time scale and pattern of decay is an order of magnitude longer to what has been observed in primary motor cortex [67,68]. In the motor cortex, SHPD does not contribute to the ongoing activity of those neurons after 100 ms and reflects the refractory and recovery periods of those motor neurons. Thus, these differences likely reflect the excitatory recurrent network connectivity of PFC networks and the time scale on which these cortical networks must maintain information to perform their requisite neurocomputations. Furthermore, the current results suggest that neural codes involving SHPD are likely a complement to firing rate-based codes within the PFC. We found that CI-GLMs which account for modulation in firing rates across different task intervals were significantly better at modeling the spiking activity of the neurons. Moreover, SHPD gains were reduced by approximately 10% when the behavioral intervals are included as CI-GLM covariates, suggesting that both SHPD and components of the task account for the variance in spiking activity.

The current study also extends the idea that excitatory recursive activity within the PFC may be critical to sustain spiking activity and may act as the neurobiological basis of working memory and/or other cognitive processes occurring during these tasks [15,69–71]. Early anatomical and recent computer models have suggested that recurrent neural connections within layers II/III and V of the PFC may support recursive, sustained activity during delay periods of working memory tasks [31–35,72–74]. Together, those studies concluded that sustained discharge generated by reverberating excitatory feedback among anatomically connected networks of neurons during delay periods is the realization of maintaining past stimuli and events, attentional processes, and abstract task rules [13–15,18,75]. However, a large body of research further implicates AMPA and NMDA receptors and intrinsic calcium-dependent mechanisms in the generation and preservation of delay-related sustained discharge [56]. Specifically, the decay of NMDA currents are generally in the range of >80 ms, but some components require seconds to decay [76], suggesting that NMDA channels and associated maintenance of excitatory currents could explain the maintenance of delay-related sustained discharge. Thus, although the current study confirms that spiking history contributes to PFC neuronal discharge activity, the precise network or cellular mechanisms underlying SHPD remains to be identified. Moreover, the timescale of SHPD for p_i PFC neurons could result from a combination of intracellular intrinsic calcium-dependent mechanisms [56,69,76–78], recurrent excitatory connections between neighboring neurons [13,32,34], as well as long recurrent paths between other cortical and subcortical brain regions, which remains to be tested.

The Effects of Stress on PFC Neural Activity

The current study found that acute noise stress increased medial PFC neuron discharge rates during delay periods of rats performing a T-maze task of spatial working memory. In contrast, a number of prior observations predicted that during stress, high levels of extracellular catecholamines were likely to result in a suppression delay related firing rates. During acute stress, NE and DA neurotransmission in the PFC is elevated, activating low-affinity noradrenergic α_1 - and β -receptors as well as the dopamine D_1 -receptor [23,26,27,30]. Activation of α_1 receptors in the PFC has been shown to suppress delay-related sustained discharge to specific cued target directions during working memory tasks [24].

Similarly, high levels of D_1 activation in the PFC suppresses delay-related activity to cued and non-cued target directions [29]. Extensive evidence suggests that the discrepancy between this prior prediction and the current observations is most likely due to stress-related increases in glutamate/glucocorticoid signaling within the PFC during acute stress [19–22]. Nonetheless, stress increases signaling within the PFC of a number of neuromodulators that may also contribute to changes in PFC neural activity during stress [79]. Increased delay-related discharge rates could reflect that, during stress, competing patterns of activation are instantiated across PFC neural populations during delay-periods that contribute to a disruption of working memory and sustained attention. Such interpretation of these data is supported by recent findings that a stress-related peptide, corticotrophin releasing factor, and activation of α_1 - receptors likely facilitates behavioral flexibility and processes involving attentional shifting [79,80].

Although delay-related neuronal discharge rates are an important measure of PFC function, neural codes involving SHPD are also likely important for computations driving cognitive/behavioral processes in a number of cortical regions, including the PFC. In the current study, we demonstrate that stress impairs SHPD, principally during delay periods. These observations are consistent with theories that stress likely impairs the ability of PFC neurons/networks to continually update and maintain information necessary for appropriate behavioral responses through the delay period [7,13,32,34,36,56,81]. For example, it has been hypothesized that stress-related increases in NE and DA neurotransmission within the PFC act to modulate intracellular cyclic adenosine monophosphate signaling and hyperpolarization-activated cyclic nucleotide-gated channel function thereby disconnecting PFC neurons from excitatory recurrent feedback [18]. Thus, regulation of recurrent excitatory activation within PFC recurrent circuitry [31,39] or regulation of NMDA related intracellular mechanisms [21,35] may underlie the current findings that stress impairs SHPD and the ability of p_i PFC neurons to retain representations of past events over time.

Lastly, we found that during the response phase of the task, firing rates of PFC neurons were suppressed during noise stress. Such actions are likely important for the complex repertoire of effects of acute stress across a range of cognitive functions. Suppression of PFC activity during the behavioral response could suggest that during stress, the PFC fails to appropriately inhibit behaviors mediated by other brain regions such as the dorsomedial striatum [82]. Such a loss of behavioral inhibition is supported by observations that habit-based actions, requiring little working memory, are favored under conditions of acute stress [40]. Furthermore, these data also support recent findings that rats prefer choices in decision-making tasks that require the least amount of work for reward following acute stress [83]. During the response phase of the task, SHPD interaction gains were enhanced at short intervals and suppressed at long intervals during acute stress. Such enhancement of short interval gains may reflect PFC activity patterns generated in the absence of ongoing inputs that could result in uncertainty/ambiguity of goal selection [84]. Additionally, it is possible that suppression of SHPD generated from spiking events in the distant past (i.e. >1.5 seconds) by stress could reflect impairment of the maintenance of information from the delay period into the response interval. Brain regions outside the PFC, including the dorsomedial striatum, could use PFC neural codes involving SHPD to guide selection of appropriate behavioral responses towards a rewarded goal. Nonetheless, the current findings are highly consistent with studies demonstrating that acute stress impairs cognitive functions requiring the PFC, whereas functions not dependent on the PFC such as hippocam-

pal- and amygdala-related processes may be facilitated with stress [18].

Summary

In summary, these results provide the first evidence that stress impairs the ability of past spiking activity to predict or modulate ongoing activity within PFC neuronal networks during delay periods of working memory tasks. Regardless of whether spike history-predicted discharge reflects an intracellular [18,35] or neural circuit mechanism [31,39], the current observations suggest that stress impairs the ability of PFC neurons/networks to continually update and maintain information through the delay period likely necessary for appropriate behavioral responses. Outside of the delay period, we conjecture that stress-related changes in spike history gain during the response period could represent inappropriate network reactivation related to an inappropriate goal selection [84,85] or uncertainty/ambiguity of goal selection. Combined, these studies identify broad effects of stress on PFC neuronal activity that likely represent a key aspect of the neurophysiological bases of stress-related cognitive impairment.

Materials and Methods

Animals

Five male Sprague-Dawley rats (300–400 g; Charles River, Wilmington MA) were individually housed in an enriched environment (Nylabone® chews) on a 13/11-hour light-dark cycle (light 0600–2000). Animals were maintained on a restricted feeding schedule (15–20 g of standard chow available immediately after training/testing). All procedures were in accordance with NIH guidelines and were approved by the University of Wisconsin Institutional Animal Care and Use Committee.

Behavioral Training/Testing

Training. Animals were trained in a T-maze delayed-non-match to position task as described previously (**Fig. 1E**; overall dim, 90 cm wide×65 cm long; runway dim 10 cm wide×10 cm high) [30]. Initial training was complete when animals entered the T-maze arm opposite from the last one visited for food rewards (chocolate chips 1.6 gm) delivered by the experimenter's hand with 90% accuracy on 10 trials (0 seconds delay, 1 session/day). Animals were then surgically implanted with recording electrodes and returned to *ad lib* feeding for the duration of recovery (7–10 days). Following recovery, training continued until animals performed two sessions of 41 trials at criterion of 90–100% correct for 2 consecutive days. Sessions were separated by 2 hours to minimize reward satiation/decreased motivation and carbohydrate-induced changes in cognitive function [86]. Importantly, no differences in performance existed between the first and second sessions. Although animals had learned the task, over time, performance in this task gradually improves at a given delay. To maintain baseline performance near 90% correct, the duration of the delay period was increased for each animal as necessary, ranging from 10–40 sec, and a new stable baseline was determined. Olfactory and visual cues were minimized by wiping the maze between each trial with 10% ethanol and lining the walls of the testing suite with black matt cloth. Masking white noise (60 db), measured at the intersection of the T (A-weighted; 2232, Brüel & Kjer Nærum Denmark), was generated from a speaker 2 meters above the center of the maze. During training sessions, animals were tethered to a dummy wire harness of identical weight and flexibly as the harness used for electrophysiological recording on testing days. After acclimation to the tether, animals showed no

differences in maze performance or overt behaviors from prior reports [30].

Testing. On the morning of testing, an animal was placed in his home cage, on top of the T-maze, 2 hours before the first session began to allow the animal to habituate to the tether and the recording arena and allowed the experimenter to discriminate neural activity. Although animals had access to water and were able to freely move about their cage, during this period animals predominantly slept. The first session (Baseline), was conducted in an identical manner to prior testing days (41 trials, 60 db white noise; **Video S1**). During the second testing session of the day, presentation of the white noise (93 db) stressor was begun immediately prior to testing and presented continuously throughout the duration of the 41 trials. White noise as stressor has been shown previously to impair PFC-dependent functions in rats, monkeys, and humans [38,48,51,57,63] and activate the stress-related circuits within the brain as well as the hypothalamic-pituitary axis of rats [49]. Testing with noise stress was permitted at most 1/week.

Surgery and Neural Data Collection

Under halothane anesthesia (Halocarbon Laboratories, River Edge, New Jersey; 1%–4% in air), animals were implanted bilaterally with linear electrode arrays (n = 8 electrodes/array; 250 μ m separation; SB103, NB Labs, Dennison, TX) targeting layer V of the prelimbic region of the PFC (p_l PFC) as previously described [52]. Electrode arrays contained 50 μ m stainless-steel electrodes orientated in a rostral-caudal direction. Electrodes were attached to skull screws (MX-0080-16B-C, Small Parts, Inc.) with dental acrylic (Plastics One, Roanoke, Virginia), the wound was closed with wound clips (9 mm Autoclip; BD Diagnostic Systems, Sparks, Maryland), and animals were allowed to recover for 7–10 days.

On testing days, animals were brought into the T-maze testing room and tethered to the Multichannel electrophysiology Acquisition Processor (MAP, Plexon, Dallas, Texas). During the 2 hour habituation period, putative single “units” of the p_l PFC were discriminated in real time using online template matching algorithms to preliminarily discriminate action potentials exhibiting a 3:1 signal to noise ratio. Following discrimination of p_l PFC units, animals remained tethered to recording hardware and the quality of the discrimination was monitored throughout the remainder of the day. During baseline and noise stress conditions, neural activity was simultaneously amplified, discriminated, time stamped, and recorded from these putative single units of the p_l PFC as previously described [46,52]. Additionally, video recordings were made of animal behavior during testing sessions (resolution = 0.0125 sec) with time-stamp overlays synchronized to the electrophysiological hardware. During the 2-hour inter-session interval, animals remained tethered and neuronal activity was monitored for drift in the quality of discrimination of action potentials.

Histology

At the end of the study, animals were deeply anesthetized and cathodal current (60 μ A) was passed across microwire pairs within a bundle for 45 sec. Animals were perfused with a 10% formalin + 5% potassium ferrocyanide solution that produced a Prussian blue reaction product at the electrode tip. Brains were removed and immersed in 10% formalin for 24 hr. Frozen 40- μ m coronal sections were collected through the p_l PFC and counterstained with Neutral Red. Representative placements of recording electrode bundles within the p_l PFC are illustrated in **Fig. 1C**.

Spike Train Analysis

Data pre-conditioning. After each day of recording, pre-established offline criteria were used to verify that waveforms assigned to each discriminated “unit” originated from a single neuron (**Fig. 1D**). These previously described criteria [46,52] were based on unit waveform properties and spike train discharge patterns including: 1) variability of peak waveform voltage, 2) variability of waveform slope(s) from peak to peak, 3) separability of clustering of scattergram points from the waveform’s first two principal components, and 4) refractory period evident in the spike train auto-correlogram. Neurons that met these criteria were further classified as “wide spike” (WS-type) or “narrow spike” (NS) to putatively identify large projection pyramidal neurons (WS-type) [53]. Essentially, the peak-peak (P-P) duration of waveforms from verified neurons were calculated. Neurons with P-P intervals greater than 200 μ s were classified as WS-type neurons. Other cells classified as NS neurons (P-P intervals between 100–200 μ s) or neurons not meeting either category were eliminated from further analyses. Lastly, p_1 PFC neuron action potential shape, neuron discharge pattern (inter-spike interval) and response properties were further examined to verify that neurons were not recorded across multiple recording sessions. Although our unpublished data indicate neurons recorded from multiple session days (separated by a week) occurs infrequently, if identified, analyses of data was limited to the first recording session of that neuron.

Behavioral events of the T-maze task were identified by visually scoring the time-stamped video recordings and manually entered into each neural recording data file. These events included 1) placement of the rat into the start box, 2) removal of the start gate, 3) rat reaching the branch point of the “T”, 4) the rat entering one of two goal arms (choice), 5) receipt of food reward, and 6) removal of the rat from the maze (**Fig. 1**). The intervals between these events were used to generate PETH’s or as predictor variables included in the CI-GLM and defined respectively as the 1) Delay interval, 2) Run interval - running down the main arm of the maze, 3) Branch interval - orienting to the left/right arm, 4) Choice interval - complete entry into one arm, 5) Reward interval - consumption of reward, 6) Pickup interval - experimenter returning animal to start box. Additionally, each trial was further classified as a correct or incorrect trial, by the chosen spatial goal (i.e. left vs. right arm), and whether it occurred during the baseline or noise stress recording session. For analyses involving interaction terms included in the CI-GLM, we extended the delay to include the pickup interval in this analysis since the pickup also likely represents a segment of the delay period and that the maximal amount of data was needed to calculate the large number of interaction terms included in the CI-GLM. Additionally for analyses involving interaction terms, we defined the behavioral response interval as the group of contiguous behavioral intervals that include the Run, Branch, and Choice. Together, these behavioral response intervals represent the response to navigate the T-maze in an attempt to acquire a reward.

Data analyses. Spike train activity was characterized by either PETH analysis or by fitting conditional intensity functions to neural spike train data using generalized linear models [41–45] to describe the effects of stress on SHPD (NeuroExplorer, Nex Technologies, NC and custom Matlab functions; Mathworks, Natick, MA). These analyses were limited to correct trials, given that few error trials occurred during baseline testing sessions and reliable estimates of neuronal spiking activity were difficult to obtain for error trials.

T-maze task-related patterns of discharge for individual neurons were initially analyzed with trial-by-trial bin counts (5 ms bins)

collected during baseline and noise stress conditions. For each recording session, trial bin counts corresponding to each behavioral interval within a trial were summarized as a temporally normalized PETH and quantified. Temporal normalization of PETH’s was necessary because, across trials of a session each behavioral interval type (e.g. Run) was comprised of different durations of time. The mean discharge rate of a neuron, calculated for each behavioral interval during stress conditions, was then represented as percent of the baseline recording session discharge rate (first recording session of the day). For all recorded neurons, a one-way ANOVA analysis (TaskComponent – behavioral interval) was performed on these normalized PETH-generated data. False Discovery Rate (FDR)-corrected single sample T-tests were used to determine that discharge rates during each behavioral interval were significantly different from values of 100.

A CI-GLM was also used to directly analyze the effects of noise stress on T-maze task interval-related patterns of discharge for each neuron. The conditional intensity function $\lambda(t|H_t)$ completely describes a neuronal point process [87]. Where λ is the estimated generalization of the rate function of a Poisson process at time (t) and $H(t)$ encompasses a number of covariates that the intensity function is conditioned upon. To fit the conditional intensity function to PFC neuron discharge, a Poisson - generalized linear model (GLM) framework was used [42–44,55,88–92]. During an evaluation step, we found that neither a homogeneous Poisson model ($\lambda(t|H_t) = \exp\{\mu\}$; **Fig. 6A**) or an inhomogeneous Poisson model ($\lambda(t|H_t) = \exp\{\mu + \beta_1 X_t^{Delay} + \beta_2 X_t^{Response}\}$; **Fig. 6B**) that included the intercept and T-maze behavior intervals as covariates could adequately fit the spike train data with a GLM. However, a conditional intensity model estimated as a function of spike history combined with each behavioral interval using the final model parameters (10th order autoregressive filter and 250 ms binning) ($\lambda(t|H_t) = \exp\{\mu + \sum_{k=1}^{10} \gamma \Delta N_{t-k} + \beta_1 X_t^{Delay} + \beta_2 X_t^{Response}\}$ **Fig. 6C**) fit spike trains well, as determined by visual assessment and quantitatively with a Kolmogorov–Smirnov (K-S) goodness-of-fit test (**Fig. 6D and Fig. S3**). The first model used to determine the overall effects of stress on SHPD was

$$\lambda_{(Model1a)}(t|H_t) = \exp\{\mu + \beta_1 X_t^{Baseline} + \vec{B}X_t^{Interval} + \sum_{k=1}^{10} (\alpha_k X_t^{Baseline} + \eta_k X_t^{Stress}) \Delta N_{t-k}\}.$$

The conditional intensity function $\lambda(t|H_t)$ was predicted for each p_1 PFC neuron from a series of covariates where (μ) is the intercept of the equation representing the background level of activity. (X_t) is a given manipulation (e.g. Baseline/Stress) for each sample in time (t). As such, the overall effect of the manipulation (Baseline/Stress) $\beta_1 X_t^{Baseline}$ or each of the T-maze behavioral intervals $\vec{B}X_t^{Interval}$ could be represented by these model covariates. β and B represent the fitted parameters for the manipulation covariate and matrix of behavioral interval covariates. Differences between left and right trials were not distinguished with this model. Spiking history during baseline or noise stress conditions $\sum_{k=1}^{10} (\alpha_k X_t^{Baseline} + \eta_k X_t^{Stress}) \Delta N_{t-k}$, is the change in the number of spiking events ΔN at one of 10 discretized time points in the past (ΔN_{t-k}). The fitted parameters for coefficients for this tenth order autoregressive process during baseline and stress are (α_k, η_k). A

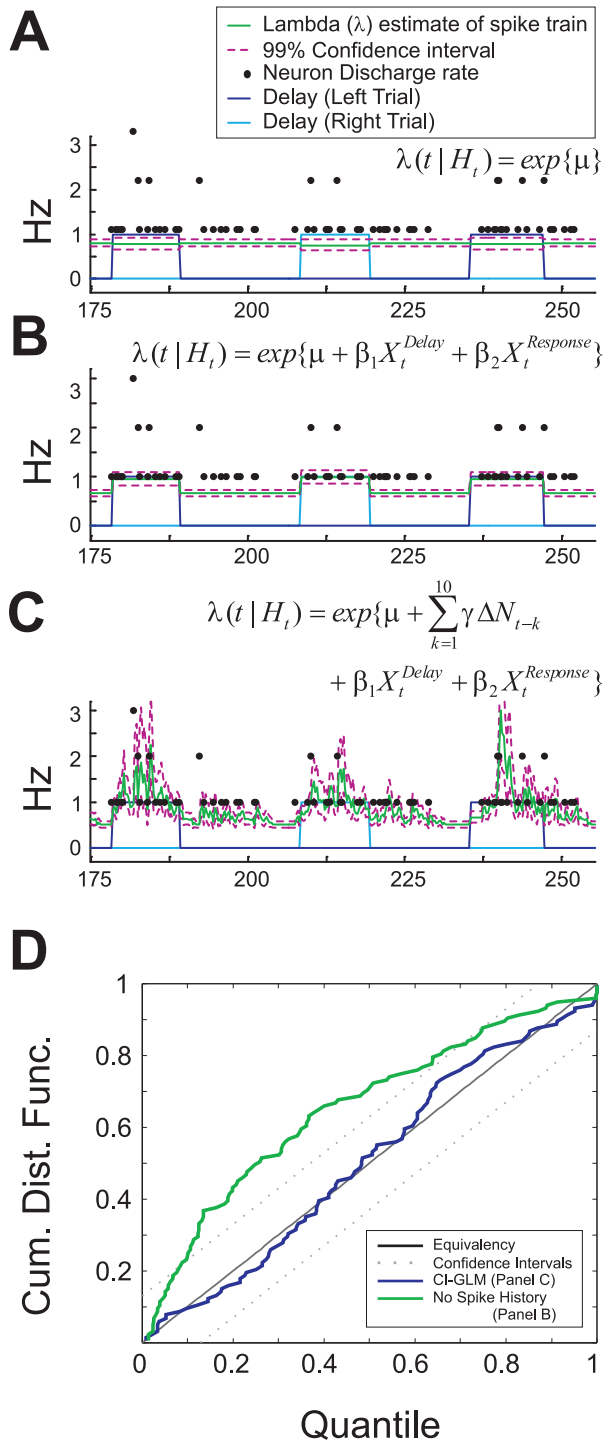


Figure 6. Characterization of generalized linear models of task-related activity. Plot of 80 seconds of spike train data, spanning three trials and fit with a GLM using (A) a homogeneous Poisson model, (B) an inhomogeneous Poisson model, and (C) an a conditional intensity model (Model 1b, during baseline conditions only). Spike counts of the original spike train are plotted with black dots against lambda (λ ; green line with red confidence intervals). X-axis=experimental time. (D) Kolmogorov-Smirnov (K-S) goodness-of-fit plot demonstrates that incorporation of spike history improves performance of the CI-GLM (blue vs. green line). The K-S plot of the final model (blue line; model from panel C) falls within equivalency confidence intervals of the K-S test (diagonal solid and dotted lines) for all quantiles, indicating that inclusion of spike history with behavioral intervals in the CI-GLM is

critical to appropriately model pPFC spiking activity. Inhomogeneous Poisson models using solely the behavioral states of the task overestimate neuron interspike intervals (green line; model from panel B). Models of neuronal activity (1–3; main text) also passed K-S goodness-of-fit tests (Fig. S3).
 doi:10.1371/journal.pcbi.1002681.g006

more parsimonious expression of this model,

$$\lambda_{(Model1b)}(t|H_t) = \exp\{\mu + \beta_1 X_t^{Baseline} + \sum_{k=1}^{10} (\alpha_k X_t^{Baseline} + \eta_k X_t^{Stress}) \Delta N_{t-k}\}$$

was also used to determine the overall effects of stress on SHPD. Given the animal always occupied one of the T-maze behavioral states $\bar{B}X_t^{Interval}$ could be collapsed to simply $\beta_1 X_t^{Baseline}$. The deviance test (likelihood ratio test) was used to compare these nested models for each neuron.

An interaction between spike history and the behavioral components of the task was then determined with the following two models:

$$\lambda_{(Model2)}(t|H_t) = \exp\{\mu + \sum_{k=1}^{10} \gamma_k \Delta N_{t-k} + \beta_1 X_t^{Baseline} + \beta_2 X_t^{Delay} X_t^{Baseline} + \beta_3 X_t^{Delay} X_t^{Stress} + \sum_{k=1}^{10} (\alpha_k X_t^{Delay} X_t^{Baseline} + \eta_k X_t^{Delay} X_t^{Stress}) \Delta N_{t-k}\}$$

and

$$\lambda_{(Model3)}(t|H_t) = \exp\{\mu + \sum_{k=1}^{10} \gamma_k \Delta N_{t-k} + \beta_1 X_t^{Baseline} + \beta_2 X_t^{Response} X_t^{Baseline} + \beta_3 X_t^{Response} X_t^{Stress} + \sum_{k=1}^{10} (\alpha_k X_t^{Response} X_t^{Baseline} + \eta_k X_t^{Response} X_t^{Stress}) \Delta N_{t-k}\}.$$

For these models, the main effects include the background level of activity (μ), the overall effect of spiking history $\sum_{k=1}^{10} \gamma_k \Delta N_{t-k}$, and the overall effect of the manipulation (Baseline/Stress; $\beta_1 X_t^{Baseline}$). Additionally, the effect of baseline vs. noise stress for a given behavioral interval of the T-maze task (extended Delay, Response interval) was also modeled (e.g. $\beta_2 X_t^{Delay} X_t^{Baseline} + \beta_3 X_t^{Delay} X_t^{Stress}$) with β_q as the estimated weighting parameters. The interaction terms of Model 2 and 3 include the product of the autoregressive process, individual behavioral intervals of the T-maze task, and Baseline/Stress conditions represented by $\sum_{k=1}^{10} \alpha_k X_t^{Delay} X_t^{Baseline} \Delta N_{t-k} + \sum_{k=1}^{10} \eta_k X_t^{Delay} X_t^{Stress} \Delta N_{t-k}$, where α_k, η_k are the estimated weighting parameters of the interaction terms. Importantly, models 2 and 3 examine the interaction with the extended Delay period vs. Response period in separate models.

The degree to which the CI-GLM output (λ) reflects the spiking activity of each p_i PFC neuron was determined by visual assessment and quantitatively with a Kolmogorov–Smirnov (K-S) goodness-of-fit test (Fig. 6D). Because the interaction models are not nested they could not be directly compared using the deviance test. However, a measure of “spiking gain”, equivalent to the rate-ratio (exponentiated covariate weights i.e. β , α , η) [54], representing the fold-change in predicted discharge activity given all other spiking activity occurring during the T-maze task was used to determine the effects of stress on SHPD. Statistical differences between the baseline recording session and noise stress were determined with a two way repeated measures ANOVA analysis (rmANOVA; Experimental Condition*Spike History Time) performed on SHPD gains. LSD post-hoc tests were used to make comparisons between individual groups. False Discovery Rate (FDR)-corrected single sample T-tests were used to determine that spiking rates or gains were significantly different from values of 1.0.

Supporting Information

Figure S1 Stress-related changes in p_i PFC neuron spike-history predicted discharge (SHPD) throughout baseline and acute stress conditions quantified using Model 1b. **A)** SHPD at different points back in time decay exponentially under baseline and stress conditions for the same ensemble of neurons used for Model 1a. For this reduced model, which did not explicitly represent all behavioral intervals, stress also produced a significant reduction in SHPD gains (main effect) without significantly alter the decay of gains at any spike history time bin. **B)** Histogram plots of calculated GLM deviance for each neuron using Models 1a (top) and 1b (bottom). For the majority of neurons, the measure of deviance was significantly reduced by incorporating behavioral intervals into the model. (EPS)

Figure S2 Action potential waveforms of 5 discriminated and validated p_i PFC neurons and rejected electrical activity. Neuronal

action potential waveforms and clusters in principal component space (inset) are replotted from Fig. 1E. Additionally, unsorted activity is included. Importantly, rejected activity includes both unsorted spiking activity and muscle artifacts including chewing. Waveform width = 450 μ s. (TIF)

Figure S3 Kolmogorov–Smirnov test plots of p_i PFC time-rescaled spike trains. Each panel represents K-S plots from each of six p_i PFC neurons from three separate animals. The solid black diagonal line represents equivalency between the actual p_i PFC spike train and $\lambda(t|H_t)$ from the CI-GLM model. Dotted lines represent the 95% confidence intervals for equivalency measures. Inclusion of spiking history covariates into the model (blue line; Model 1a of main text) significantly improves $\lambda(t|H_t)$ estimations from models that only include behavioral intervals (green line, model from Fig. 6B). (EPS)

Video S1 Video clip of electrophysiological recording while performing the T-maze task. Three trials are shown, a left-correct, a right-correct, and a right-incorrect. The green inset text denotes the animal ID, experimental time, and video frame number. (MOV)

Acknowledgments

The authors would like to thank Robert C. Spencer and Tim Stellick for help in collecting these data. Additionally, the authors would like to thank Robert C. Spencer for his insightful comments in preparing this manuscript.

Author Contributions

Conceived and designed the experiments: DMD CWB. Performed the experiments: DMD. Analyzed the data: DMD. Contributed reagents/materials/analysis tools: DMD RLJ. Wrote the paper: DMD CWB. Designed the analysis and wrote the Matlab code: DMD RLJ.

References

- Kolb B (1990) Prefrontal cortex. In: Kolb B, Tees RC, editors. The cerebral cortex of the rat. Cambridge, MA: MIT.
- Romanides AJ, Duffy P, Kalivas PW (1999) Glutamatergic and dopaminergic afferents to the prefrontal cortex regulate spatial working memory in rats. *Neuroscience* 92: 97–106.
- Sanchez-Santed F, de Bruin JP, Heinsbroek RP, Verwer RW (1997) Spatial delayed alternation of rats in a T-maze: effects of neurotoxic lesions of the medial prefrontal cortex and of T-maze rotations. *Behav Brain Res* 84: 73–79.
- Spencer RC, Klein RM, Berridge CW (2012) Psychostimulants Act Within the Prefrontal Cortex to Improve Cognitive Function. *Biol Psychiatry* 72: 221–227.
- Arnsten AF, Li BM (2005) Neurobiology of executive functions: catecholamine influences on prefrontal cortical functions. *Biol Psychiatry* 57: 1377–1384.
- Funahashi S, Bruce CJ, Goldman-Rakic PS (1989) Mnemonic coding of visual space in the monkey's dorsolateral prefrontal cortex. *J Neurophysiol* 61: 331–349.
- Fuster JM, Alexander GE (1971) Neuron activity related to short-term memory. *Science* 173: 652–654.
- Kubota K, Niki H (1971) Prefrontal cortical unit activity and delayed alternation performance in monkeys. *J Neurophysiol* 34: 337–347.
- Ramos BP, Arnsten AF (2007) Adrenergic pharmacology and cognition: focus on the prefrontal cortex. *Pharmacol Ther* 113: 523–536.
- Chudasama Y, Muir JL (2001) Visual attention in the rat: a role for the prefrontal cortex and thalamic nuclei? *Behav Neurosci* 115: 417–428.
- Passetti F, Chudasama Y, Robbins TW (2002) The frontal cortex of the rat and visual attentional performance: dissociable functions of distinct medial prefrontal subregions. *Cereb Cortex* 12: 1254–1268.
- Batuev AS, Kursina NP, Shutov AP (1990) Unit activity of the medial wall of the frontal cortex during delayed performance in rats. *Behav Brain Res* 41: 95–102.
- Goldman-Rakic PS (1995) Cellular basis of working memory. *Neuron* 14: 477–485.
- Lebedev MA, Messinger A, Kralik JD, Wise SP (2004) Representation of attended versus remembered locations in prefrontal cortex. *PLoS Biol* 2: e365.
- Miller EK, Cohen JD (2001) An integrative theory of prefrontal cortex function. *Annu Rev Neurosci* 24: 167–202.
- Haber SN, Knutson B (2010) The reward circuit: linking primate anatomy and human imaging. *Neuropsychopharmacology* 35: 4–26.
- Watanabe M (1996) Reward expectancy in primate prefrontal neurons. *Nature* 382: 629–632.
- Arnsten AF (2009) Stress signalling pathways that impair prefrontal cortex structure and function. *Nat Rev Neurosci* 10: 410–422.
- Jackson ME, Moghaddam B (2006) Distinct patterns of plasticity in prefrontal cortex neurons that encode slow and fast responses to stress. *Eur J Neurosci* 24: 1702–1710.
- Lowy MT, Gault L, Yamamoto BK (1993) Adrenalectomy attenuates stress-induced elevations in extracellular glutamate concentrations in the hippocampus. *J Neurochem* 61: 1957–1960.
- Moghaddam B (1993) Stress preferentially increases extraneuronal levels of excitatory amino acids in the prefrontal cortex: comparison to hippocampus and basal ganglia. *J Neurochem* 60: 1650–1657.
- Yuen EY, Liu W, Karatsoreos IN, Feng J, McEwen BS et al. (2009) Acute stress enhances glutamatergic transmission in prefrontal cortex and facilitates working memory. *Proc Natl Acad Sci U S A* 106: 14075–14079.
- Arnsten AF, Mathew R, Ubriani R, Taylor JR, Li BM (1999) Alpha-1 noradrenergic receptor stimulation impairs prefrontal cortical cognitive function. *Biol Psychiatry* 45: 26–31.
- Bimbaum SG, Yuan PX, Wang M, Vijayraghavan S, Bloom AK et al. (2004) Protein kinase C overactivity impairs prefrontal cortical regulation of working memory. *Science* 306: 882–884.
- Devilbiss DM, Waterhouse BD (2000) Norepinephrine exhibits two distinct profiles of action on sensory cortical neuron responses to excitatory synaptic stimuli. *Synapse* 37: 273–282.
- Finlay JM, Zigmond MJ, Abercrombie ED (1995) Increased dopamine and norepinephrine release in medial prefrontal cortex induced by acute and chronic stress: effects of diazepam. *Neuroscience* 64: 619–628.

27. Roth RH, Tam SY, Ida Y, Yang JX, Deutch AY (1988) Stress and the mesocorticolimbic dopamine systems. *Ann N Y Acad Sci* 537: 138–147.
28. Joels M (2006) Corticosteroid effects in the brain: U-shape it. *Trends Pharmacol Sci* 27: 244–250.
29. Vijayraghavan S, Wang M, Birnbaum SG, Williams GV, Arnsten AF (2007) Inverted-U dopamine D1 receptor actions on prefrontal neurons engaged in working memory. *Nat Neurosci* 10: 376–384.
30. Zahrt J, Taylor JR, Mathew RG, Arnsten AF (1997) Supranormal stimulation of D1 dopamine receptors in the rodent prefrontal cortex impairs spatial working memory performance. *J Neurosci* 17: 8528–8535.
31. Amit DJ (1995) The hebbian paradigm reintegrated - Local reverberations as internal representations. *Behav Brain Sci* 18: 617–626.
32. Arnsten AF, Paspalas CD, Gamo NJ, Yang Y, Wang M (2010) Dynamic Network Connectivity: A new form of neuroplasticity. *Trends Cogn Sci* 14: 365–375.
33. Goldman-Rakic PS (1987) Circuitry of the primate prefrontal cortex and the regulation of behavior by representational memory. In: Plum F, editors. *The nervous system: Higher functions of the brain*. Bethesda, MD: American Physiological Society. pp. 373–417.
34. Hebb, D O. (1949) *The organization of behavior: A neurophysiological theory*. New York: Wiley.
35. Mongillo G, Barak O, Tsodyks M (2008) Synaptic theory of working memory. *Science* 319: 1543–1546.
36. Wang XJ (2001) Synaptic reverberation underlying mnemonic persistent activity. *Trends Neurosci* 24: 455–463.
37. Yuen EY, Liu W, Karatsoreos IN, Ren Y, Feng J et al. (2011) Mechanisms for acute stress-induced enhancement of glutamatergic transmission and working memory. *Mol Psychiatry* 16: 156–170.
38. Arnsten AF (2000) Stress impairs prefrontal cortical function in rats and monkeys: role of dopamine D1 and norepinephrine alpha-1 receptor mechanisms. *Prog Brain Res* 126: 183–192.
39. Arnsten AF (2011) Prefrontal cortical network connections: key site of vulnerability in stress and schizophrenia. *Int J Dev Neurosci* 29: 215–223.
40. Schwabe L, Wolf OT (2011) Stress-induced modulation of instrumental behavior: from goal-directed to habitual control of action. *Behav Brain Res* 219: 321–328.
41. Brown EN, Frank LM, Tang D, Quirk MC, Wilson MA (1998) A statistical paradigm for neural spike train decoding applied to position prediction from ensemble firing patterns of rat hippocampal place cells. *J Neurosci* 18: 7411–7425.
42. Paninski L, Pillow JW, Simoncelli EP (2004) Maximum likelihood estimation of a stochastic integrate-and-fire neural encoding model. *Neural Comput* 16: 2533–2561.
43. Truccolo W, Eden UT, Fellows MR, Donoghue JP, Brown EN (2005) A point process framework for relating neural spiking activity to spiking history, neural ensemble, and extrinsic covariate effects. *J Neurophysiol* 93: 1074–1089.
44. Jenison RL, Rangel A, Oya H, Kawasaki H, Howard MA (2011) Value encoding in single neurons in the human amygdala during decision making. *J Neurosci* 31: 331–338.
45. Eden UT (2008) Point Process Models for Neural Spike Trains. In: Mitra P, editors. *Neural Signal Processing: Quantitative Analysis of Neural Activity*. Washington, DC: Society for Neuroscience.
46. Devilbiss DM, Berridge CW, Jenison RL (2011) Conditional intensity/point process model of task-related prefrontal spiking: effects of performance. *BMC Neuroscience* 12: 160.
47. Amemiya S, Yanagita S, Suzuki S, Kubota N, Motoki C et al. (2010) Differential effects of background noise of various intensities on neuronal activation associated with arousal and stress response in a maze task. *Physiol Behav* 99: 521–528.
48. Berridge CW, Jenison RL, Devilbiss DM (2010) Impact of stress on performance and task-related information represented by neurons of the prefrontal cortex in rat using a conditional intensity/point-process model. 805.7. San Diego, CA: Society for Neuroscience.
49. Buraw A, Day HE, Campeau S (2005) A detailed characterization of loud noise stress: Intensity analysis of hypothalamo-pituitary-adrenocortical axis and brain activation. *Brain Res* 1062: 63–73.
50. Helfferich F, Palkovits M (2003) Acute audiogenic stress-induced activation of CRH neurons in the hypothalamic paraventricular nucleus and catecholaminergic neurons in the medulla oblongata. *Brain Res* 975: 1–9.
51. Arnsten AF, Goldman-Rakic PS (1998) Noise stress impairs prefrontal cortical cognitive function in monkeys: evidence for a hyperdopaminergic mechanism. *Arch Gen Psychiatry* 55: 362–368.
52. Devilbiss DM, Berridge CW (2008) Cognition-enhancing doses of methylphenidate preferentially increase prefrontal cortex neuronal responsiveness. *Biol Psychiatry* 64: 626–635.
53. Bartho P, Hirase H, Monconduit L, Zugaro M, Harris KD et al. (2004) Characterization of neocortical principal cells and interneurons by network interactions and extracellular features. *J Neurophysiol* 92: 600–608.
54. Dobson, A J. (2002) *An Introduction to Generalized Linear Models*. Boca Raton: Chapman & Hall/CRC Press.
55. Truccolo W, Hochberg LR, Donoghue JP (2010) Collective dynamics in human and monkey sensorimotor cortex: predicting single neuron spikes. *Nat Neurosci* 13: 105–111.
56. Durstewitz D (2009) Implications of synaptic biophysics for recurrent network dynamics and active memory. *Neural Netw* 22: 1189–1200.
57. Holmes A, Wellman CL (2009) Stress-induced prefrontal reorganization and executive dysfunction in rodents. *Neurosci Biobehav Rev* 33: 773–783.
58. Kesner RP, Farnsworth G, Dimattia BV (1989) Double Dissociation of Egocentric and Allocentric Space Following Medial Prefrontal and Parietal Cortex Lesions in the Rat. *Behav Neurosci* 103: 956–961.
59. Mishkin M (1964) Perseveration of central sets after frontal lesions in monkeys. In: Warren JM, Akert K, editors. *The frontal granular cortex and behavior*. New York: McGraw-Hill. pp. 219–241.
60. Messinger A, Lebedev MA, Kralik JD, Wise SP (2009) Multitasking of attention and memory functions in the primate prefrontal cortex. *J Neurosci* 29: 5640–5653.
61. Shafi M, Zhou Y, Quintana J, Chow C, Fuster J et al. (2007) Variability in neuronal activity in primate cortex during working memory tasks. *Neuroscience* 146: 1082–1108.
62. Jung MW, Qin Y, McNaughton BL, Barnes CA (1998) Firing characteristics of deep layer neurons in prefrontal cortex in rats performing spatial working memory tasks. *Cereb Cortex* 8: 437–450.
63. Arnsten AFT, Robbins TW (2002) Neurochemical modulation of prefrontal cortical function in humans and animals. In: Stuss DT, Knight RT, editors. *Principles of Frontal Lobe Function*. New York: Oxford University Press.
64. Hains AB, Vu MA, Maciejewski PK, van Dyck CH, Gottron M et al. (2009) Inhibition of protein kinase C signaling protects prefrontal cortex dendritic spines and cognition from the effects of chronic stress. *Proc Natl Acad Sci U S A* 106: 17957–17962.
65. Shansky RM, Rubinow K, Brennan A, Arnsten AF (2006) The effects of sex and hormonal status on restraint-stress-induced working memory impairment. *Behav Brain Funct* 2: 8.
66. Romanski LM, Goldman-Rakic PS (2002) An auditory domain in primate prefrontal cortex. *Nat Neurosci* 5: 15–16.
67. Stevenson IH, Rebecco JM, Hatsopoulos NG, Haga Z, Miller LE et al. (2009) Bayesian inference of functional connectivity and network structure from spikes. *IEEE Trans Neural Syst Rehabil Eng* 17: 203–213.
68. Truccolo W, Friehs GM, Donoghue JP, Hochberg LR (2008) Primary motor cortex tuning to intended movement kinematics in humans with tetraplegia. *J Neurosci* 28: 1163–1178.
69. Compte A (2006) Computational and in vitro studies of persistent activity: edging towards cellular and synaptic mechanisms of working memory. *Neuroscience* 139: 135–151.
70. Durstewitz D, Seamans JK (2006) Beyond bistability: biophysics and temporal dynamics of working memory. *Neuroscience* 139: 119–133.
71. Hazy TE, Frank MJ, O'Reilly RC (2006) Banishing the homunculus: making working memory work. *Neuroscience* 139: 105–118.
72. Gabbott PL, Dickie BG, Vaid RR, Headlam AJ, Bacon SJ (1997) Local-circuit neurons in the medial prefrontal cortex (areas 25, 32 and 24b) in the rat: morphology and quantitative distribution. *J Comp Neurol* 377: 465–499.
73. Metz AE, Yau HJ, Centeno MV, Apkarian AV, Martina M (2009) Morphological and functional reorganization of rat medial prefrontal cortex in neuropathic pain. *Proc Natl Acad Sci U S A* 106: 2423–2428.
74. Zhang ZW (2004) Maturation of layer V pyramidal neurons in the rat prefrontal cortex: intrinsic properties and synaptic function. *J Neurophysiol* 91: 1171–1182.
75. Mongillo G, Amit DJ, Brunel N (2003) Retrospective and prospective persistent activity induced by Hebbian learning in a recurrent cortical network. *Eur J Neurosci* 18: 2011–2024.
76. Spruston N, Jonas P, Sakmann B (1995) Dendritic glutamate receptor channels in rat hippocampal CA3 and CA1 pyramidal neurons. *J Physiol* 482 (Pt 2): 325–352.
77. Franssen E, Tahvildari B, Egorov AV, Hasselmo ME, Alonso AA (2006) Mechanism of graded persistent cellular activity of entorhinal cortex layer v neurons. *Neuron* 49: 735–746.
78. Lisman JE, Fellous JM, Wang XJ (1998) A role for NMDA-receptor channels in working memory. *Nat Neurosci* 1: 273–275.
79. Snyder K, Wang WW, Han R, McFadden K, Valentino RJ (2012) Corticotropin-releasing factor in the norepinephrine nucleus, locus coeruleus, facilitates behavioral flexibility. *Neuropsychopharmacology* 37: 520–530.
80. Berridge CW, Shumsky JS, Andrzejewski ME, McGaughy JA, Spencer RC et al. (2012) Differential sensitivity to psychostimulants across prefrontal cognitive tasks: differential involvement of noradrenergic alpha- and alpha-receptors. *Biol Psychiatry* 71: 467–473.
81. Hopfield JJ (1982) Neural networks and physical systems with emergent collective computational abilities. *Proc Natl Acad Sci U S A* 79: 2554–2558.
82. Gregoire S, Rivalan M, Le MC, lu-Hagedorn F (2011) The synergy of working memory and inhibitory control: Behavioral, pharmacological and neural functional evidences. *Neurobiol Learn Mem* 97: 202–12.
83. Shafiei N, Gray M, Viau V, Floresco SB (2012) Acute Stress Induces Selective Alterations in Cost/Benefit Decision-Making. *Neuropsychopharmacology*. Epub ahead of print.
84. Bogacz R, Gurney K (2007) The basal ganglia and cortex implement optimal decision making between alternative actions. *Neural Comput* 19: 442–477.
85. Botvinick MM, Niv Y, Barto AC (2009) Hierarchically organized behavior and its neural foundations: a reinforcement learning perspective. *Cognition* 113: 262–280.

86. McNay EC, Gold PE (2002) Food for thought: fluctuations in brain extracellular glucose provide insight into the mechanisms of memory modulation. *Behav Cogn Neurosci Rev* 1: 264–280.
87. Daley DJ, Vere-Jones D (2003) *An Introduction to the Theory of Point Processes*. New York: Springer.
88. Smith AC, Brown EN (2003) Estimating a state-space model from point process observations. *Neural Comput* 15: 965–991.
89. Eden UT, Frank LM, Barbieri R, Solo V, Brown EN (2004) Dynamic analysis of neural encoding by point process adaptive filtering. *Neural Comput* 16: 971–998.
90. Paninski L (2006) The most likely voltage path and large deviations approximations for integrate-and-fire neurons. *J Comput Neurosci* 21: 71–87.
91. Paninski L (2004) Maximum likelihood estimation of cascade point-process neural encoding models. *Network* 15: 243–262.
92. Marjoram P, Molitor J, Plagnol V, Tavaré S (2003) Markov chain Monte Carlo without likelihoods. *Proc Natl Acad Sci U S A* 100: 15324–15328.